N90-10101

A PERFORMANCE COMPARISON OF INTEGRATION ALGORITHMS IN SIMULATING FLEXIBLE STRUCTURES

By

R. M. Howe
The University of Michigan
Applied Dynamics International
Ann Arbor, Michigan

ABSTRACT

Modeling of the dynamic vibration modes of a flexible structure can be achieved either by using a generalized coordinate for each mode considered in the simulation, or by discretizing the structure into a sufficiently large number of segments to provide the necessary modal accuracy. The accuracy and stability considerations in choosing appropriate numerical integration algorithms are different, depending on which modeling approach is utilized. In the generalized coordinate approach the frequency and shape of each mode is assumed to be known. The integration method should provide an accurate match to the modal frequency and damping, and should also exhibit sinusoidal transfer function errors which are acceptably small, especially for frequencies in the vicinity of the modal resonance. Since only those modes considered necessary for the required simulation fidelity are included as generalized coordinates, integrator stability for modes of higher frequency does not become in an issue.

On the other hand, when the discretized structure approach is used, high frequency modes not of interest to the simulation will nevertheless be present. In this case it is important that the integration method not only provide satisfactory characteristic root and transfer function accuracy for the lower modes of interest, but also provide stable solutions with satisfactory damping for the higher modes which are not of interest.

In this paper asymptotic formulas for the characteristic root errors as well as transfer function gain and phase errors are presented for a number of traditional integration methods and for several new integration methods. Normalized stability regions in the λh plane are compared for the various methods. In particular, it is shown that a modified form of Euler integration with root matching is an especially efficient method for simulating lightly-damped structural modes. The method has been used successfully for structural bending modes in the real-time simulation of missiles. Performance of this algorithm is compared with other special algorithms, including the state-transition method. A predictor-corrector version of the modified Euler algorithm permits it to be extended to the simulation of nonlinear models of the type likely to be obtained when using the discretized structure approach.

Performance of the different integration methods is also compared for integration step sizes larger than those for which the asymptotic formulas are valid. It is concluded that many traditional integration methods, such as RD-4, are not competitive in the simulation of lightly damped structures.

A Performance Comparison of Integration Algorithms in Simulating Flexible Structures

R. M. Howe

The University of Michigan, Ann Arbor, Michigan

and

Applied Dynamics International, Ann Arbor, Michigan

ABSTRACT

In this paper a number of integration algorithms, including several new methods, are considered for the simulation of flexible structures. The effectiveness of the different algorithms is assessed by considering the characteristic root errors which they produce, the sinusoidal transfer function gain and phase errors, the stability regions, and the execution times. The suitability of the various algorithms for simulations with real-time inputs is also noted. When the structural modes in a simulation are represented by generalized (normal) coordinates, the selection criteria for integration methods are somewhat different than the criteria when the structure is discretized into a sufficiently large number of segments to provide the necessary modal accuracy. In this paper asymptotic formulas for the characteristic root errors as well as transfer function gain and phase errors are presented for a number of traditional integration methods and for several new integration methods. Normalized stability regions in the λh plane are compared for the various methods. In particular, it is shown that a modified form of Euler integration with root matching is an especially efficient method for simulating structural modes. The method has been used successfully for structural bending modes in the real-time simulation of missiles. A predictor version of the modified Euler algorithm permits it to be extended to the simulation of nonlinear models of the type likely to be obtained when using the discretized structure approach.

1. Introduction

Modeling of the dynamic vibration modes of a flexible structure can be achieved either by using a generalized coordinate for each mode considered in the simulation, or by discretizing the structure into a sufficiently large number of segments to provide the necessary modal accuracy. In this latter case the mathematical model for a flexible structure with N degrees of freedom has the following general form:

$$M(q)\ddot{q} + C(q,\dot{q}) + K(q) = F(t) \qquad (1)$$

where q is an N-component position state vector, $M(q)$ is the mass matrix, $C(q,\dot{q})$ is the coriolis and centrifugal acceleration vector, $K(q)$ is the elastic and gravity force vector, and $F(t)$ is the external force vector. When the vibration modes of the structure are represented by normal

(generalized) coordinates, a coordinate x representing the time-varying amplitude of a given mode with undamped natural frequency ω_n and damping ratio ζ obeys the equation

$$\ddot{x} + 2\zeta\omega_n\dot{x} + \omega_n^2 x = \omega_n^2 \phi(t) \qquad (2)$$

Here $\phi(t)$ is the generalized force associated with the coordinate x. When a number of modes are present, there will in general also be terms in Eq. (2) which couple the mode of amplitude x with other structural modes.

The accuracy and stability considerations in choosing appropriate numerical integration algorithms for solving differential equations of the type shown in (1) or (2) will be different. In the generalized coordinate approach of Eq. (2) the frequency and shape of each mode is assumed to be known. The integration method should provide an accurate match to the modal frequency and damping, and should also exhibit sinusoidal transfer function errors which are acceptably small, especially for frequencies in the vicinity of the modal resonance. Since only those modes considered necessary for the required simulation fidelity are included as generalized coordinates, integrator stability for higher frequency modes which are not of interest does not become an issue.

On the other hand, when the discretized structure approach represented by Eq. (1) is used, high frequency modes which are unimportant in the simulation will nevertheless be present. In this case it is important that the integration method not only provide satisfactory characteristic root and transfer function accuracy for the lower modes of interest, but also provide stable solutions with satisfactory damping for the higher modes which are not of interest.

In this paper asymptotic formulas for the characteristic root errors as well as transfer function gain and phase errors are presented for a number of traditional integration methods and for several new integration methods. Normalized stability regions in the λh plane are compared for the various methods, where λ is an eigenvalue asociated with the linearized perturbation equations of the structure and h is the integration step size. . In particular, it is shown that a modified form of Euler integration with root matching is an especially efficient method for simulating lightly-damped structural modes. The method has been used successfully for structural bending modes in the real-time simulation of missiles. Predictor versions of the modified Euler algorithm permit it to be extended to the simulation of nonlinear models of the type likely to be obtained when structures are represented by means of discretization. The stability regions in the λh plane for the modified Euler methods are especially well suited to the requirements when using the discretized structure approach.

2. Dynamic Error Measures for Integration Algorithms

In comparing different integration methods for the simulation of flexible structures it is important to utilize meaningful performance measures which permit general conclusions to be drawn regarding the expected dynamic errors associated with each method. Our dynamic error analysis will be based on linearized perturbation equations derived from the original nonlinear differential equations used to model the structure. Thus we will assume that the system

eigenvalues are known, as well as the transfer functions relating specific input-output pairs. We will further assume that the simulation uses a fixed integration step size h. This is necessary in the case of a real-time simulation. It is likely to be true over a large number of steps even when a variable-step integration method is used in simulating a flexible structure. For linearized equations and a fixed integration step size we can apply the method of z transforms to anayze the dynamic errors resulting from specific integration algorithms [1,2]. There are two error measures which quite useful in predicting overall dynamic accuracy in the simulation. The first is the fractional error in each characteristic root (eigenvalue) of the digital simulation, defined as

$$\text{Fractional error in characteristic root } = e_\lambda = \frac{\lambda^* - \lambda}{\lambda} \tag{3}$$

where λ is the characteristic root of the continuous system being simulated and λ^* is the equivalent characteristic root for the digital simulation. For the case of complex roots (of which there will be many conjugate pairs in the simulation of a flexible structure) it is more appropriate to determine the fractional error, e_ω, in root frequency and the damping ratio error, e_ζ. Thus we define

$$e_\omega = \frac{\omega_d^* - \omega_d}{\omega_d} \quad , \quad e_\zeta = \zeta^* - \zeta \tag{4}$$

Here ω_d^* and ω_d represent the frequencies of the digital and continuous system roots, respectively, while ζ^* and ζ represent the damping ratios for the digital and continuous system roots, respectively.

The second dynamic error measure of significance is the fractional error in digital system transfer function for sinusoidal inputs of frequency ω. For any input-output pair let $H(s)$ be the transfer function of the continuous system and $H^*(z)$ be the z transform of the digital system that results when a particular integration algorithm is used. Then the fractional error in sinusoidal transfer function is given by [3]

$$\frac{H^*(e^{j\omega h})}{H(j\omega)} - 1 = e_M + je_A \tag{5}$$

For simulations of any reasonable accuracy the magnitude of this fractional error will be small compared with unity, in which case it is easily shown that the real part, e_M, is equal approximately to the fractional error in gain and the imaginary part, e_A, is equal to the phase error of the transfer function [3].

For any numerical integration algorithm the integrator transfer function for sinusoidal inputs of frequency ω can be written approximately as [3]

$$H_I^*(e^{j\omega h}) \cong \frac{1}{j\omega h \left[1 + e_I(j\omega h)^k \right]} \quad , \quad \omega h \ll 1 \tag{6}$$

499

where h is the integration step size. Since $1/(j\omega h)$ is the ideal integrator transfer function, it is apparent that the term $e_I(j\omega h)^k$ represents the integrator error. For Adams-Bashforth predictor and Adams-Moulton two-pass predictor-corrector algorithms of order 2, 3, and 4, integration methods that are candidates for simulation of flexible structures, the error coefficient e_I and algorithm order k are listed in Table 1.

Table 1. Integrator Transfer Function Error Parameters for AB Predictor and AM Predictor Corrector Algorithms

Method	Error Coefficient, e_I	Algorithm Order, k
AB-2	$\dfrac{5}{12}$	2
AB-3	$\dfrac{3}{8}$	3
AB-4	$\dfrac{251}{720}$	4
AM-2	$\dfrac{1}{12}$	2
AM-3	$\dfrac{1}{24}$	3
AM-4	$\dfrac{19}{720}$	4

In terms of e_I and k the following formula for e_λ, the fractional error in characteristic root as defined earlier in Eq. (3), can be derived [3]:

$$e_\lambda = \frac{\lambda^* - \lambda}{\lambda} \cong -e_I(\lambda h)^k \quad , \qquad |\lambda h| << 1 \tag{7}$$

It is apparent that e_λ is directly proportional to the integrator error coefficient, e_I. For complex characteristic roots equivalent asymptotic formulas for the root frequency and damping errors, e_ω and e_ζ, as defined in Eq. (4), can be derived [3]. As in Eq. (7), the errors are proportional to $e_I|\lambda h|^k$.

For digital simulation of a first order system with transfer function $H(s) = 1/(s-\lambda)$ the fractional error in the transfer function for sinusoidal inputs, as defined in Eq. (5), can also be derived in terms of the integrator error parameters e_I and k [3]. From this result the following asymptotic formulas are obtained for e_M, the fractional error in transfer function gain, and e_A, the transfer function phase error:

For k odd, $e_M \cong (-1)^{\frac{k+1}{2}} \dfrac{\omega \lambda e_I}{\omega^2 + \lambda^2} (\omega h)^k$, $e_A \cong (-1)^{\frac{k+1}{2}} \dfrac{\omega^2 e_I}{\omega^2 + \lambda^2} (\omega h)^k$, $\omega h \ll 1$ \hspace{1em} (8)

For k even, $e_M \cong -(-1)^{\frac{k}{2}} \dfrac{\omega^2 e_I}{\omega^2 + \lambda^2} (\omega h)^k$, $e_A \cong (-1)^{\frac{k}{2}} \dfrac{\omega \lambda e_I}{\omega^2 + \lambda^2} (\omega h)^k$, $\omega h \ll 1$ \hspace{1em} (9)

Here the errors are proportional to $e_I(\omega h)^k$. Comparable asymptotic formulas for e_M and e_A can be derived for digital simulation of a second-order system with transfer function $H(s) = 1/(s^2 + 2\zeta\omega_n s + \omega_n^2)$ [3]. Again, the gain and phase errors are proportional to $e_I(\omega h)^k$.

The transfer function $H(s)$ for any order linear system with both real and complex roots can be represented as the product of first and second-order transfer functions. In this case it can be shown that the asymptotic formulas for the digital system transfer function gain and phase errors is simply the sum of the individual first and second-order subsystem gain and phase errors, respectively, for predictor and predictor-corrector methods of the type shown in Table 1. If we simulate a flexible structure with a given integration method, this permits us to compute the linearized system gain and phase errors at the frequency ω for any input-output pair as a function of integration step size h. In view of the reemerging popularity of frequency-domain methods for designing multiple input/multiple output control systems, this is a quite useful result. It permits us to estimate ahead of time for a given step size and integration method whether the simulation errors will be satisfactorily small. Conversely, for a given transfer function accuracy requirement, it allows us to compute the maximum allowable step size h for the simulation.

It should be noted that the methodology outlined above for determining characteristic root and transfer function errors for any order of linearized system from the simple integrator model given by Eq. (6) does not work in the case of multiple-pass, single step methods such as Runge-Kutta. This is because the results of individual passes within a single step in such methods depend on the particular form of the system transfer function. Asymptotic formulas for the root error parameters e_λ, e_ω, and e_ζ can, of course, be derived separately for RK-2, RK-3, RK-4, and variations of these methods [3].

3. Modified Euler Integration Algorithms

In this section we describe some modifications of simple Euler integration which have potential advantages over conventional integration methods such as those listed in Table 1. First we introduce the concept of state variables defined at both integer and half integer sample times. Assume that the simulation of a mechanical degree of freedom with position state x, velocity state y, and acceleration a involves integrating the following simple state equations:

$$\dot{y} = a, \quad \dot{x} = y \hspace{3em} (10)$$

501

Next assume that successive data points are defined at integer time samples in representing the acceleration a and position x, and at half-integer sample times in representing the velocity y. The following modified Euler algorithms can then be used for integration:

$$y_{n+1/2} = y_{n-1/2} + h a_n \;\; , \;\; x_{n+1} = x_n + h y_{n+1/2} \tag{11}$$

The basic concept behind this modification of standard Euler integration is very simple; instead of the using the state variable derivative defined at the beginning of the integration step, the method uses a state variable derivative defined halfway through the step. For this algorithm it is easy to show that the integrator error coefficient defined in Eq. (6) is given by $e_I = 1/24$ and the order of the method is $k = 2$. Thus the accuracy of this single-pass algorithm is twice that of the two-pass AM-2 predictor-corrector. However, the algorithm does require that the velocity states be defined at half-integer sample times.

Let us apply this modified Euler method to the second-order system represented by Eq. (2) for the generalized coordinate x. We can replace Eq. (2) by the following two state equations:

$$\dot{y} = \omega_n [\phi(t) - x - 2\zeta y] \;\; , \;\; \dot{x} = \omega_n y \tag{12}$$

By analogy with Eq. (11) the modified Euler difference equations become:

$$y_{n+1/2} = y_{n-1/2} + \omega_n h (\phi_n - x_n - 2\zeta y_n') \;\; , \;\; x_{n+1} = x_n + \omega_n h y_{n+1/2} \tag{13}$$

Since y_n is not explicitly computed, it is necessary to substitute an estimate y_n' in the damping term on the right side of the $y_{n+1/2}$ equation. There are many ways in which the y_n' estimate can be computed. In Table 2 we list four candidate methods.

Table 2. Methods for Estimating the Velocity y_n in Modified Euler Integration

Method	Formula for the Estimate, y_n'
1. Average of $y_{n+1/2}$ and $y_{n-1/2}$	$y_n' = \dfrac{y_{n+1/2} + y_{n-1/2}}{2}$
2. Extrapolation using $y_{n-1/2}$ and $y_{n-3/2}$	$y_n' = \dfrac{3}{2} y_{n-1/2} - \dfrac{1}{2} y_{n-3/2}$
3. Integration using $\dot{y}_{n-1}$ and $\dot{y}_{n-2}$	$y_n' = y_{n-1/2} + \dfrac{7}{8} \dot{y}_{n-1} - \dfrac{3}{8} y_{n-2}$
4. Estimate based on $y_{n-1/2}$	$y_n' = y_{n-1/2}$

The estimate for y_n in the first method is simply based on averaging $y_{n+1/2}$ and $y_{n-1/2}$. This is equivalent to utilizing trapezoidal integration for the damping term. Although this means that $y_{n+1/2}$ now appears on both sides of the difference equation in (13), for the linear system considered here it is possible to solve explicitly for $y_{n+1/2}$, as we will see in the next section. In the second method the estimate for y_n is based on a linear extrapolation from $y_{n-1/2}$ and $y_{n-3/2}$. This is equivalent to using trapezoidal integration for the damping term. Since $y_{n+1/2}$ now appears only on the left side of the difference equation in (13), this method can be used in the simulation of equations where dy/dt is a nonlinear function of y. This is also true for the third and fourth methods. The third is based on a second-order predictor integration over the interval $h/2$, starting with $y_{n-1/2}$ and using dy/dt at the n-1 and n-2 intervals. This is equivalent to estimating y_n with quadratic extrapolation based on $y_{n-1/2}$, $y_{n-3/2}$ and $y_{n-5/2}$. In the fourth method we simply use $y_{n-1/2}$ as our estimate for y_n. This is equivalent to Euler integration for the damping term.

4. Modified Euler Integration with Trapezoidal Damping

We have seen in Table 2 that the velocity estimate y'_n for the modified Euler difference equations in (13) can be based on the average of $y_{n+1/2}$ and $y_{n-1/2}$. Thus

$$y'_n = \frac{y_{n+1/2} + y_{n-1/2}}{2} \tag{14}$$

As noted earlier, this is equivalent to utilizing trapezoidal integration for the damping term. Although this means that $y_{n+1/2}$ now appears on both sides of the difference equation, for the linear system considered here it is possible to solve explicitly for $y_{n+1/2}$. In this way we obtain the following equations:

$$y_{n+1/2} = C_1 y_{n-1/2} + C_2 (\phi_n - x_n), \quad x_{n+1} = x_n + \omega_n h y_{n-1/2} \tag{15}$$

where

$$C_1 = \frac{1 - \zeta \omega_n h}{1 + \zeta \omega_n h}, \quad C_2 = \frac{\omega_n h}{1 + \zeta \omega_n h} \tag{16}$$

From the method of z transforms applied to Eqs. (15) and (16) we obtain the following asymptotic formulas for the frequency and damping ratio errors of the digital simulation [4]:

$$e_\omega = \frac{\omega_d^* - \omega_d}{\omega_d} \cong \frac{1 + 4\zeta^2 - 8\zeta^4}{24(1 - \zeta^2)} \omega_n^2 h^2, \quad e_\zeta = \zeta^* - \zeta \cong \frac{\zeta}{24}(4\zeta^2 - 1), \quad \omega_n h \ll 1 \tag{17}$$

The transfer function gain and phase errors are given approximately by

503

$$\text{Fractional gain error} = \frac{|H^*|}{|H|} - 1 = e_M \cong \frac{-\frac{\zeta\omega}{\omega_n}\left[1 - \frac{\omega^2}{\omega_n^2}\right]}{\left[1 - \frac{\omega^2}{\omega_n^2}\right]^2 + \left[\frac{2\zeta\omega}{\omega_n}\right]^2} (\omega h), \quad \omega h \ll 1 \tag{18}$$

$$\text{Phase error} = e_A \cong \frac{\frac{2\zeta^2\omega^2}{\omega_n^2}}{\left[1 - \frac{\omega^2}{\omega_n^2}\right]^2 + \left[\frac{2\zeta\omega}{\omega_n}\right]^2} (\omega h), \quad \omega h \ll 1 \tag{19}$$

The characteristic root errors in Eq. (17) and the transfer function gain and phase errors in Eqs. (18) and (19) are comparable with those for AM-2 integration for the same step size h [3]. Yet AM-2 is a two-pass method whereas the modified Euler with trapezoidal damping, as used here, is a single-pass method. Thus it will take only half as long to execute as AM-2 while producing comparable accuracy. Its accuracy is approximately 5 times better than the accuracy of AB-2 integration when applied to the same second-order system.

The accuracy of modified Euler integration when applied to a linear second-order system can be further improved by the technique of root matching, which was originally employed by Fowler to improve the performance of conventional Euler integration [5]. By taking the z transform of Eqs. (15) and (16) we can obtain exact analytic formulas for the undamped natural frequency ω_n^* and damping ratio ζ^* in terms of ω_n and ζ. From these formulas we can solve for ω_n and ζ in terms of ω_n^* and ζ^*. If in these formulas we then replace ω_n and ζ by ω_n' and ζ', respectively, and ω_n^* and ζ^* by ω_n and ζ, respectively, we obtain the following [4]:

$$\omega_n' = \frac{1}{h}\sqrt{2 - \frac{2\cos(\omega_n h\sqrt{1 - \zeta^2})}{\cosh(\zeta\omega_n h)}} \tag{20}$$

$$\zeta' = \frac{\tanh(\zeta\omega_n h)}{\omega_n' h} \tag{21}$$

If ω_n' and ζ' from these formulas are used instead of ω_n and ζ in Eqs. (15) and (16), the resulting digital simulation will exhibit ω_n^* and ζ^* values which exactly match the ω_n and ζ of the continuous system being simulated. For a given step size h the ω_n', ζ', C_1 and C_2 can be precomputed, so that each integration step in simulating the second-order system only requires 3 multiplies and 2 adds, as before. Now the charcteristic roots of the digital simulation will be exactly equal to those of the continuous system, regardless of the integration step size h. The approximate formulas for the transfer function gain and phase errors are given by [4]:

$$e_M \cong \frac{1}{24}(\omega h)^2 , \quad e_A \cong -\frac{\zeta \omega_n}{6\omega}(\omega_n h)^2 , \quad \omega h << 1 \qquad (22)$$

Note that the fractional error in gain, e_M, is completely independent of the damping ratio ζ, and the phase error e_A approaches zero as ζ approaches zero. Thus our modified Euler algorithm with root matching will be especially effective in simulating lightly-damped second-order systems, as will be the case in structural modes. This is illustrated in Figure 1, where gain and phase versus frequency for a second-order system with $\zeta = 0.01$ are plotted. Because of the sharp resonant peak in gain and the extremely rapid change in phase as ω passes through ω_n, it is very critical that both the natural frequency and damping ratio of the digital simulation match that of the continuous system. The table at the bottom of the figure shows the transfer function errors for input frequencies in the vicinity of ω_n for the specific case of $\omega_n h = 0.5$, which corresponds to only 2 integration steps per radian or 12.57 steps per cycle. Shown in the table are the gain and phase errors based on both an exact calculation from the system z transform, $H^*(e^{j\omega h})$, as well as the approximate formulas of Eq. (31). Note how closely the approximate caculations agree with the exact, even for the example here for which $\omega h \approx 0.5$.

Until now we have only analyzed the dynamic performance of the modified Euler method in the frequency domain. This has been accomplished by examining the gain and phase errors of the transfer function for sinusoidal inputs.We now consider the errors in computed response of the second-order system to a unit-step input. Figure 2 shows the errors which result when using RK-2 integration (Heun's method); modified Euler with trapezoidal integration for the damping term, i.e., Eqs. (15) and (16); and modified Euler with root matching, i.e., ω_n' and ζ' from Eqs. (20) and (21) substituted for ω_n and ζ in Eqs. (15) and (16). For the example in the figure the damping ratio $\zeta = 0.707$ and the integration step size is given by $\omega_n h = 0.5$. The results show that the RK-2 errors are 4 to 10 times larger than the modified Euler errors. It should also be noted that RK-2 is a two-pass method, that is, it requires two evaluations of the state-variable derivatives per integration step. It follows that RK-2 will take approximately twice as long to execute per integration step as the single-pass modified Euler methods. To provide the same output integration frame rate in real time the RK-2 method will therefore require twice the mathematical step size h in comparison with the modified Euler methods considered here. This will further increase by a factor of 4 the RK-2 errors relative to the modified Euler errors in Figure 2.

The modified Euler results shown in Figure 2 were obtained using an initial step of $h/2$ in integrating $dydt$ to obtain y. After one integration step this provides the calculation of $y_{1/2}$ starting with the initial condition y_0. The step size is taken as h for all subsequent dy/dt integration steps. This results in successive velocity values representing y at half-integer step times, consistant with the concept introduced in the beginning of this section.
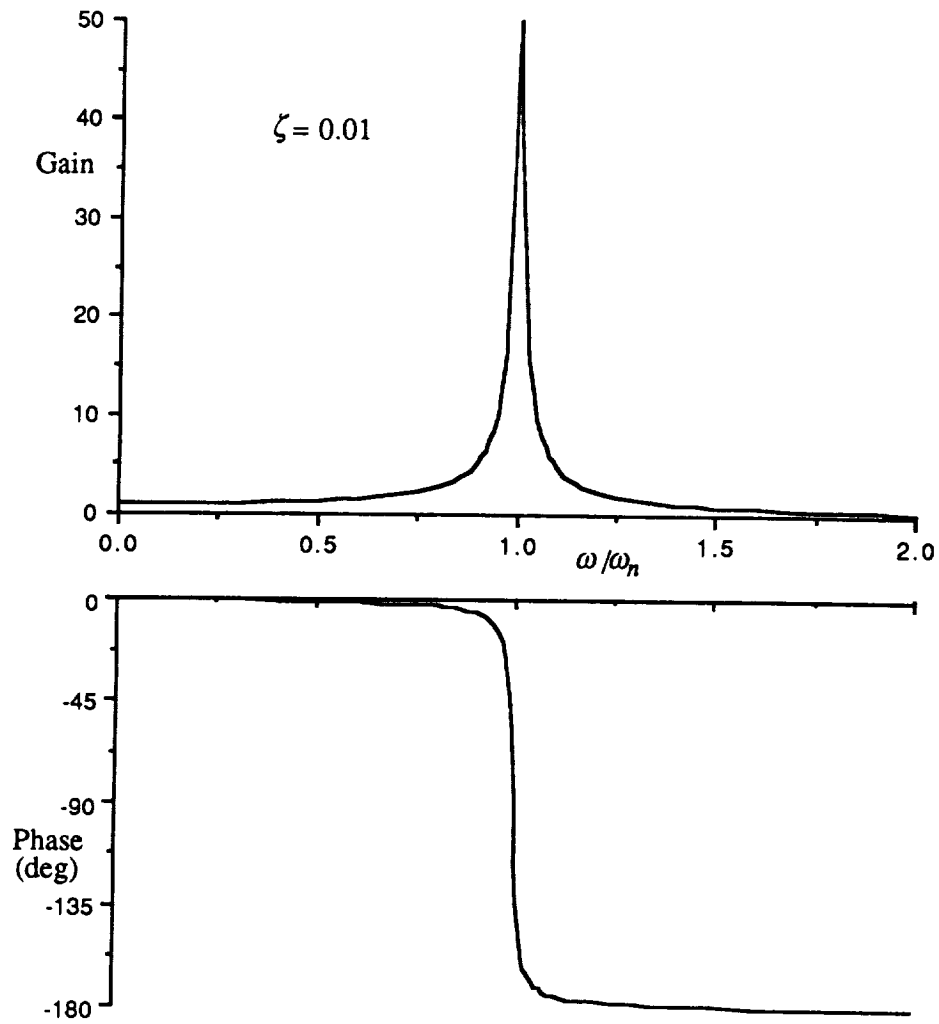
	ω/ω_n	Fractional Gain Error		Phase Error (radians)	
		Exact	Eq. (31)	Exact	Eq. (31)
$\omega_n h = 0.5$	0.7	0.01040	0.01021	-0.000296	-0.000292
	0.9	0.01727	0.01888	-0.000381	-0.000375
12.57 steps	1.0	0.02137	0.02083	-0.000424	-0.000317
per cycle)	1.1	0.02592	0.02521	-0.000467	-0.000458
	1.4	0.04240	0.04083	-0.000595	-0.000583

Figure 1. Frequency response of lightly-damped second-order system using modified Euler integration with root matching, $\omega_n h = 0.5$.
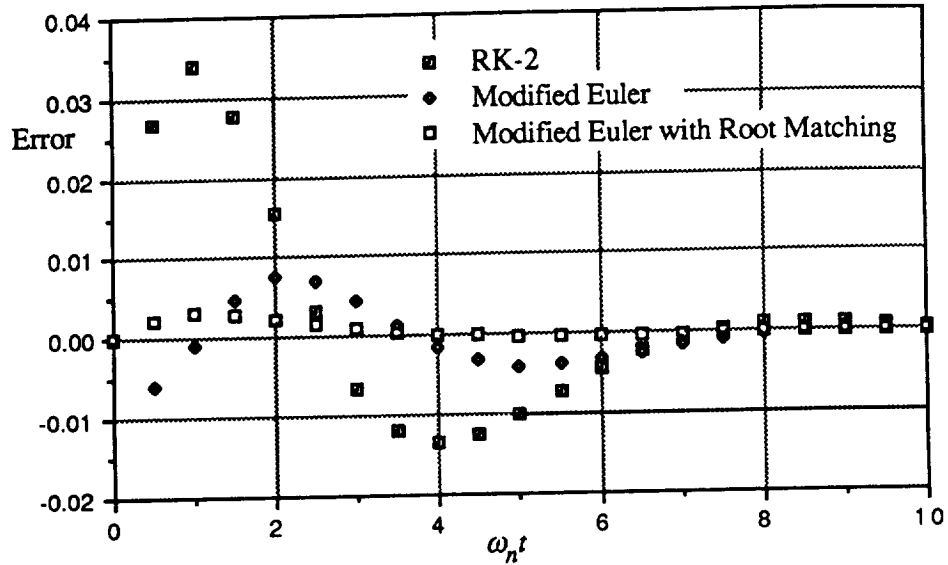
Figure 2. Unit step response errors in simulating a second-order system with damping ratio $\zeta = 0.707$, integration step size given by $\omega_n h = 0.5$.

5. Performance of Other Versions of Modified Euler Integration

In this section we present the asymptotic formulas for characteristic root and transfer function errors when modified Euler integration is used to simulate a second-order system with methods 2, 3, or 4 in Table 2 utilized to calculate the velocity estimate y_n' in Eq. (13). For method 2, which is equivalent to AB-2 integration for the damping term, the following results are obtained for e_ω, the fractional error in root frequency, and e_ζ, the damping ratio error [6]:

$$e_\omega \cong \frac{1 - 32\zeta^2 + 40\zeta^4}{24(1 - \zeta^2)}(\omega_n h)^2 \ , \qquad e_\zeta \cong \frac{11\zeta - 20\zeta^3}{24}(\omega_n h)^2 \ , \quad \omega_n h \ll 1 \qquad (23)$$

These errors are significantly less than the errors when AB-2 is used for all integrations. For method 3 in Table 2, which uses a second-order predictor integration algorithm to compute y_n', the following asymptotic formulas are obtained for the root frequency and damping errors:

$$e_\omega \cong \frac{(1 - 4\zeta^2)}{24}(\omega_n h)^2 \ , \qquad e_\zeta \cong \frac{\zeta - \zeta^3}{12}(\omega_n h)^2 \ , \quad \omega_n h \ll 1 \qquad (24)$$

The transfer function gain and phase errors are given by

507

$$e_M \cong -\frac{2\frac{\omega^2}{\omega_n^2}\left[1-2\zeta^2-\frac{\omega^2}{\omega_n^2}\right]}{\left[1-\frac{\omega^2}{\omega_n^2}\right]^2+\left[2\zeta\frac{\omega}{\omega_n}\right]^2}\frac{(\omega_n h)^2}{24} \quad , \quad e_A \cong \frac{2\zeta\frac{\omega}{\omega_n}\left[1+\frac{\omega^2}{\omega_n^2}\right]}{\left[1-\frac{\omega^2}{\omega_n^2}\right]^2+\left[2\zeta\frac{\omega}{\omega_n}\right]^2}\frac{(\omega_n h)^2}{24} \quad , \quad \omega h \gg 1$$

$$(25)$$

In both Eqs. (24) and (25) the errors are a factor of two smaller than the corresponding errors when AM-2 is used for all integrations. In addition, the AM-2 algorithm is a two-pass method which will therefore take twice as long to execute on a given computer. For method 4 in Table 2, which is equivalent to using Euler integration for the damping term, the following formulas are obtained for the characteristic root and transfer function errors [4]:

$$e_\omega \cong \frac{\frac{1}{2}\zeta-\zeta^3}{1-\zeta^2}\omega_n h \quad , \quad e_\zeta \cong \frac{1}{2}\zeta^2\omega_n h \quad , \quad \omega_n h \ll 1 \tag{26}$$

$$e_M \cong \frac{-\zeta\frac{\omega}{\omega_n}\left[1-\frac{\omega^2}{\omega_n^2}\right]}{\left[1-\frac{\omega^2}{\omega_n^2}\right]^2+\left[2\zeta\frac{\omega}{\omega_n}\right]^2}(\omega h) \quad , \quad e_A \cong \frac{2\zeta^2\frac{\omega^2}{\omega_n^2}}{\left[1-\frac{\omega^2}{\omega_n^2}\right]^2+\left[2\zeta\frac{\omega}{\omega_n}\right]^2}(\omega h) \quad , \quad \omega h \gg 1 \tag{26}$$

Note that the errors are all proportional to the first power of the step size h. This is because of the first-order Euler algorithm used for integration of the damping term. For $\zeta = 0$, however, the first-order errors in Eqs. 25) and (26) vanish, meaning that the errors become second-order in h. This is to be expected, since the conventional Euler integration plays no role when $\zeta = 0$. In fact it can be shown that when $\zeta = 0$, the digital solution will have zero damping regardless of the step size h.

When method 2,3, or 4 in Table 1 (or any other explicit method) is used to provide the estimate y_n' for the velocity state, the modified Euler method can be used as the algorithm for integrating the nonlinear state equations represented by (1). The vector difference equations become the following:

$$\dot{q}_{n+1/2} = \dot{q}_{n-1/2} + h\{F_n - [M(q_n)]^{-1}C(q_n,\dot{q}_n') - K(q_n)\} \quad , \quad q_{n+1} = q_n + h\dot{q}_{n+1/2} \tag{28}$$

We now turn to a consideration of integration algorithm stability.

6. Stability of Integration Methods

It has already been pointed out that the stability of numerical integration algorithms becomes an important consideration when the flexible structure is modeled by discretization. This is because the discretized model will contain high frequency modes which are unimportant in the simulation but can cause numerical instabilities for reasonable integration step sizes. For a given integration method the stability boundary in the λh plane can be obtained by considering a simulation of the linear system with transfer function $H(s) = 1/(s-\lambda)$. From the difference equation the z transform, $H^*(z)$, is obtained. The stability boundary is defined by the λh values for which the denominator of $H^*(z)$ vanishes when $|z| = 1$. These λh values can be obtained by letting $z = e^{j\theta}$ in the denominator of $H^*(z)$ and solving for λh for θ values ranging between 0 and π. When this is done for the AB predictor methods, the stability regions plotted in Figure 3 are obtained. The regions are symmetric with respect to the real axis so that only the upper half plane is shown. For any values of λh lying outside the boundaries the digital simulation will be unstable. In the case of both AB-3 and AB-4 the boundary crosses over into the right half plane. This means that a continuous system with roots on the imaginary axis which correspond to undamped transients can exhibit stable transients in the digital solution. Put another way, it means that AB-3 and AB-4 solutions will exhibit more damping than the continuous system being simulated. This is actually desirable in the case of the high frequency modes which are not of interest in a given simulation. On the other hand the AB predictor methods do not have particularly large stability regions and therefore do not permit very large integration step sizes h compared with the reciprocal magnitude, $1/|\lambda|$, of the largest eigenvalues in the simulation.
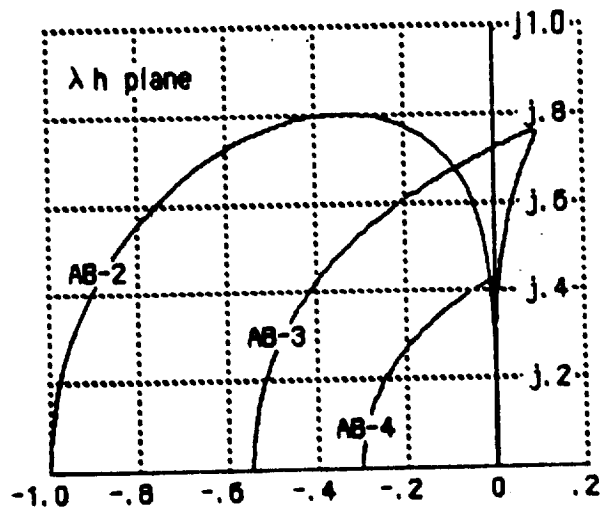

Figure 3. Stability boundaries for AB predictor integration.

In Figure 4 the stability boundaries are shown for the the two-pass AM predictor-corrector methods. Although the boundaries are considerably larger than those for the AB methods, it must be remembered that the AM algorithms will take twice as long to execute. Thus the boundaries should be reduced by a factor of two for a valid comparison with AB-2. When this

is done, the AM-2 and 3 boundaries actually fall inside the AB-2 and 3 boundaries, although the AM-4 boundary still lies outside the AB-4 boundary. In all cases the higher-order algorithms exhibit less stability and are therefore unlikely to be candidates for simulating flexible structures.
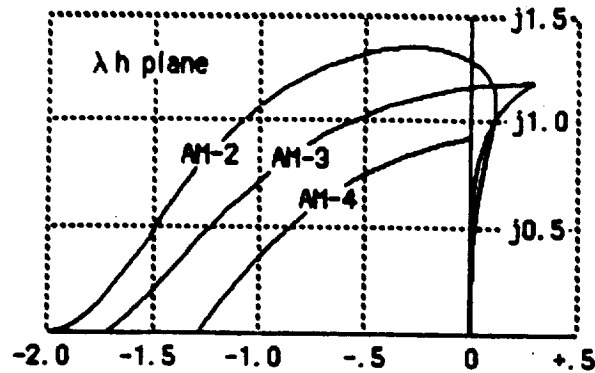

Figure 4. Stability boundaries for two-pass AM predictor-corrector integration.

For comparison purposes the stability boundaries for RK-2, 3 and 4 are shown in Figure 5. We recall that these algorithms require 2, 3 and 4 passes, respectively, through the state equations per integration step. Thus for proper comparison with single-pass methods the boundaries shown should be reduced by factors of 2, 3 and 4, respectively. When this is done, the RK-2 boundary roughly matches the AB-2 boundary, while the RK-3 and RK-4 boundaries still fall outside the AB-3 and 4 boundaries, respectively.
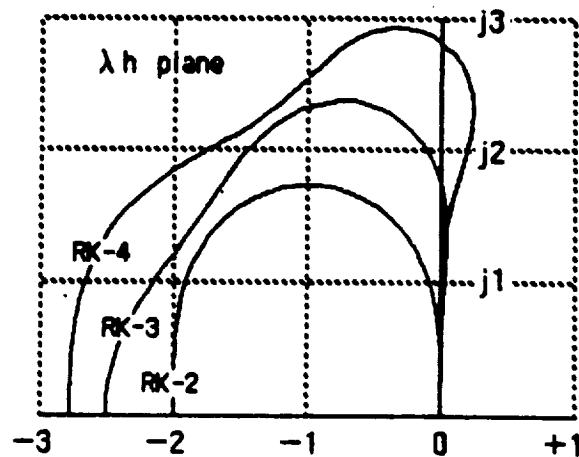

Figure 5. Stability boundaries for Runge-Kutta integration methods.

Finally, in Figure 6 are shown the stability boundaries for various modified Euler methods, as described in Sections 4 and 5. The trapezoidal damping case corresponds to method 1 in Table 2, the Euler damping case to method 4, the AB-2 damping case to method 2, and the predictor damping case to method 3. Also shown for comparison purposes in Figure 6 are the stability boundaries for AB-2, AM-2 and RK-2, as presented earlier in Figures 3, 4 and 5, respectively. The AM-2 and RK-2 stability boundaries have been reduced by a factor of two to reflect the two passes per integration step required in the implementation of these methods. Note that all four of the Modified Euler methods in Figure 6 have stability regions which permit values of $|\lambda h|$ up to 2 for lightly damped transients, e.g., eigenvalues near the imaginary axis. In this regard the methods are considerably superior to the AB-2, AM-2 and RK-2 algorithms and should perform especially well in the simulation of flexible structures.

It should also be noted that the modified Euler methods are ideally suited for real-time simulation in that they do not require inputs prior to their occurence in real time. For example, if $F(t)$ in Eq. (1) is a real time input, then the single-pass modified Euler algorithm of Eq. (28) only requires F_n at the beginning of the nth integration step. On the other hand, the AM predictor-corrector algorithms require F_{n+1} at the start of the second pass for the nth integration step, and F_{n+1} is not yet available in real time. There is, however, a modified version of the AM-2 predictor method which is compatible with real-time inputs [6]. The AB predictor methods are also compatible with real time inputs, and there are versions of RK-2 and RK-3 which permit real-time inputs [3]. RK-4 is not compatible with real-time inputs, since it requires $F_{n+1/2}$ at the beginning of the second pass and F_{n+1} at the start of the fourth pass, in both cases prior to their availability in real time.
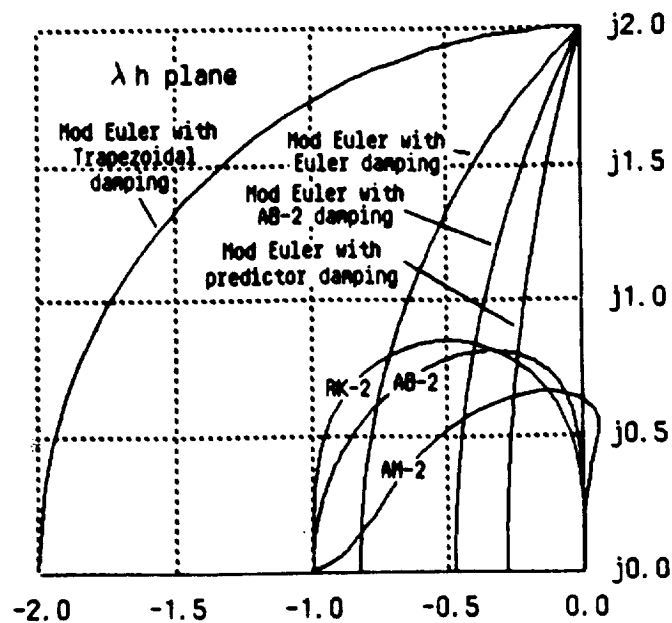

Figure 6. Stability boundaries for modified Euler integration methods.

7. Conclusions

In this paper we have considered the dynamic performance of integration methods in the context of simulating flexible structures. In terms of both characteristic root errors and transfer function errors, both important in such simulations, we have compared the performance of traditional integration methods with various versions of modified Euler integration . We have shown that modified Euler integration is especially effective in simulating lightly-damped structural modes. We have also shown that the modified Euler methods have very favorable stabilty boundaries in the λh plane with respect to requirements in the simulation of lightly-damped modes. This is especially significant when a flexible structure is modeled by discretization as opposed to normal coordinates, since it will allow larger integration step sizes before the solution goes unstable due to the presence of higher modes which are unimportant to the simulation.

References

1. Gilbert, E.G., "Dynamic Error Analysis of Digital and Combined Digital-Analog Systems," *Simulation*, vol. 6, no. 4, April 1966, pp 241-257.

2. Benyon, P.K., "A Review of Numerical Methods for Digital Simulation," *Simulation*, vol. 11, no. 4, Nov. 1968.

3. Howe, R.M., "Transfer Function and Characteristic Root Errors for Fixed-Step Integration Algorithms," *Transactions of the Society for Computer Simulation*, vol. 2, no. 4, Dec. 1985, pp 293-320.

4. Howe, R.M., "Simulation of Linear Systems Using Modified Euler Integration Methods," to appear in *Transactions of the Society for Computer Simulation*.

5. Fowler, M.E., "A New Numerical Method for Simulation," *Simulation*, vol. 4, no. 5, May 1965, pp 324-330.

6. Howe, R.M., "The Role of Modified Euler Integration in Real-Time Simulation," *Proceedings of the Conference on Aerospace Simulation II*, San Diego, 1986; pp 263-275. The Society for Computer Simulation, P.O. Box 17900, San Diego, CA 92117.

THIS PAGE INTENTIONALLY LEFT BLANK

513

OPTICAL PROCESSING FOR DISTRIBUTED SENSORS IN CONTROL OF FLEXIBLE SPACECRAFT

BY

SHARON S. WELCH, RAYMOND C. MONTGOMERY,
MICHAEL F. BARSKY, AND IAN T. GALLIMORE

NASA LANGLEY RESEARCH CENTER
SPACECRAFT CONTROL BRANCH
HAMPTON, VA 23665-5225

PRESENTATION FOR THE
WORKSHOP ON COMPUTATIONAL ASPECTS IN THE
CONTROL OF FLEXIBLE SYSTEMS
WILLIAMSBURG, VA

514